

Final Technical Report

USGS/NEHRP Award No: 07HQGR0044

**Evaluation of Double-difference Algorithms for Near-Real-Time Event
Relocation at the NEIC**

Principal Investigator: Felix Waldhauser
Co-PI: David Schaff

Lamont-Doherty Earth Observatory of Columbia University
Palisades, NY 10964
Tel: (845) 365 8538; Fax: (845) 365 8150
felixw@ldeo.columbia.edu

Project Period: 01/01/2007 – 12/31/2007 (NFE: -12/31/2008)

Research supported by the U.S. Geological Survey (USGS), Department of the Interior, under USGS award number 07HQGR0044. The views and conclusions contained in this document are those of the authors and should not be interpreted as necessarily representing the official policies, either expressed or implied, of the U.S. Government.

USGS/NEHRP Award No: 07HQGR0044

Evaluation of Double-difference Algorithms for Near-Real-Time Event Relocation at the NEIC

Principal Investigator: Felix Waldhauser
Co-PI: David Schaff

Lamont-Doherty Earth Observatory of Columbia University
Palisades, NY 10964
Tel: (845) 365 8538; Fax: (845) 365 8150
felixw@ldeo.columbia.edu

SUMMARY

We tested and evaluated global cross-correlation and double-difference algorithms for their potential implementation at the NEIC to relocate earthquakes recorded at global seismic stations on a routine basis. Specifically, we developed, applied, and evaluated time-domain cross-correlation methods to improve differential times based on phase picks. We applied the new tools to seismograms of subduction zone events beneath northern Chile and crustal earthquakes in the 1999 Izmit and Düzce, Turkey, aftershock sequences. We find a high level of waveform similarity in the subduction seismicity, and a low level of waveform similarity in the Turkey aftershock sequence. The Turkey aftershock sequence, consequently, has few correlated events, which we attribute to the complexity of both the fault structures and faulting processes. Nevertheless, double-difference solutions based on a combination of differential times from cross-correlation and EHB phase picks are able to image orientation and dip of individual fault segments that are consistent with focal mechanisms and near surface information. Differences between the double-difference locations and corresponding locations in global seismicity catalogs (EDR, ISC, EHB) are typically greater than 10 km. Residual statistics and comparison with accurately known locations from local network data indicate mean relative location errors at the 90% confidence level of 2.4 km laterally and 1.8 km vertically. These results indicate that cross-correlation and double-difference methods may be useful to obtain high-resolution event locations within the framework of routine earthquake catalog production at the NEIC. Support from this grant has therefore also been used to perform additional work beyond the proposed tasks towards the over-arching goal of global real-time DD relocations at the NEIC. Specifically, research has been performed towards the generation of global high-resolution background seismicity catalogs.

1. Project overview

This report covers the activities performed between January 1, 2007 (start date of the project) and December 31, 2008 (NFE from 1/1/2008-12/13/2008) on evaluating the general applicability of global double-difference algorithms to relocate earthquakes in the framework of routine catalog production at the NEIC. Under this grant (07HQGR0044) we focused on the use of cross-correlation methods to improve on arrival time picks. This project was a continuation of a previous project (05HQGR0175; 1/2006-12/2006) with the same general research goal but with the focus on adapting the hypoDD algorithm of Waldhauser (2001) for use with phase pick data from the NEIC. Note that in the final project report of the previous grant 05HQGR0175 we have also included part of the work carried out under this grant. Thus work specific to this grant has been repeated in this report. In addition, we describe additional work supported by this grant (but not originally proposed) that we carried out towards the over-arching goal of global real-time DD relocation. The work described here is being undertaken by the principle investigator Felix Waldhauser and by co-PI David Schaff.

2. Investigations undertaken

Waveform Cross Correlation of Regional and Teleseismic Seismograms

We have developed efficient cross-correlation algorithms to compute accurate differential arrival times for globally observed phases of pairs of closeby events recorded at common stations. Cross-correlation methods take advantage of the fact that two earthquakes that are close in space and have similar focal mechanisms produce similar seismograms at common stations (Poupinet et al., 1984). Cross-correlation methods can then measure differential phase arrival times with sub-sample precision, typically resulting in more than an order of magnitude improvement over phase onset picks in earthquake bulletins (e.g., Poupinet et al., 1984; Schaff et al., 2004). Since the double-difference method (Waldhauser and Ellsworth, 2000) uses differential times directly, events with correlated seismograms are relocated to the accuracy of the cross-correlation data while events that do not correlate are determined to the accuracy of the phase pick data.

The new tools, described in more detail in Waldhauser and Schaff (2007), are based on time domain cross correlation algorithms that we successfully applied to local earthquake data (Schaff et al., 2004; Schaff and Waldhauser, 2005), regional phases (Schaff and Richards, 2005; Waldhauser et al., 2004), and teleseismic phases of small number of earthquakes (Zhang et al., 2005; Zhang et al., 2007) and nuclear explosions (Waldhauser et al., 2004). We reworked these tools so they can be applied to large numbers of earthquakes and stations, using waveforms obtained from IRIS and recorded at stations around the world. We have implemented STA/LTA filters that precede the correlations in order to reduce the number of noise-correlations and improve the robustness of the differential time measurements. This has proven especially useful when using theoretical predictions to find the arrival times of the phases we like to correlate in cases where there are not picks in the bulletin.

The performance of these new cross-correlation tools is best shown using an example of 359 events that occurred in the subducting Nazca plate beneath Northern Chile. We performed 56,621 ‘black-box’ cross correlations at 998 stations, from which 7318 P- and 567 S-waves have a cross correlation coefficient (CC) > 0.7. The cross correlations were performed on a 10 s window surrounding the first arriving P- or S-waves. Lags searched over are plus and minus 5 s. Examples of cross-correlated seismograms are shown in Figure 1 for phases observed at regional

(station ZOBO, Bolivia) and teleseismic (ANMO, USA; WMQ, China) distances. Superimposed on the aligned waveforms are the EHB bulletin phase picks that demonstrate the two main benefits of using waveform cross correlation: the reduction in the scatter in phase onset picks (ZOBO, WMQ), and the measurement of additional delay times of phases not picked by analysts. The standard deviation of the scatter in the analyst picks is 1.7 s at station ZOBO, 0.14 s at station WMQ, and 0.03 s at station ANMO (note that station ANMO has only two picks). Errors in the correlation measurements based on an evaluation of the internal consistency is on the order of 0.01 s or less. For WMQ this represents about one order and for ZOBO two orders of magnitude improvement over differential times formed from phase picks. The improvement in differential time accuracy translated to relative location errors of 2 km horizontally and 1.4 vertically for correlated events, compared to an average of 3.5 km and 2.1 km when all double-difference locations are considered (Waldhauser and Schaff, 2007). Median horizontal and vertical location differences between our cross-correlation based double-difference locations and the ISC locations are 15 and 132 km, respectively. Differences to the EHB locations are 12 km in both directions, within the range of the estimated average EHB location uncertainty (10-15 km, Engdahl et al., 1998).

In the following we present an application to earthquakes most crucial to the NEIC, i.e. crustal earthquakes such as in the 1999 Izmit/Düzce aftershock sequence, and demonstrate performance and location precision using ‘ground truth’ events, focal mechanisms, and near surface information.

3. Results from crustal earthquake relocation

We choose 75 crustal events in the 1999 Izmit-Düzce earthquake sequence to investigate the performance of the global cross-correlation based double-difference algorithm to relocate hypocenters in the Earth’s crust. The events span a distance of nearly 200 km along the northernmost strand of the North Anatolian fault system, making them well suited to investigate the effect of fault structure, interevent distances, and waveform similarity on double-difference solutions. The Izmit Mw 7.4 mainshock occurred on 17 August 1999 and was centered at 40.748 N., 29.864 E at a depth of 17 km (USGS). It ruptured approximately 60 km of the surface in an almost pure right lateral strike slip fashion (USGS CMT: strk=95, dip=81, slip=180; Harvard CMT: strk=91, dip=87, slip=164). On 12 November 1999 a second earthquake with Mw 7.1 occurred about 100 km to the east of the Izmit event near the village of Düzce, at 40.758 N 31.161 E and 10 km depth (USGS). Again, CMT solutions indicate almost pure right lateral strike slip (USGS CMT: strk=269, dip=73, slip=177; Harvard CMT: strk=268, dip=54, slip=167). These two mainshocks and 40 aftershocks ($3.8 < M_w < 5.8$) from the Izmit event and 33 aftershocks ($4.0 < M_w < 5.5$) from the Düzce event are used in our relocation analysis.

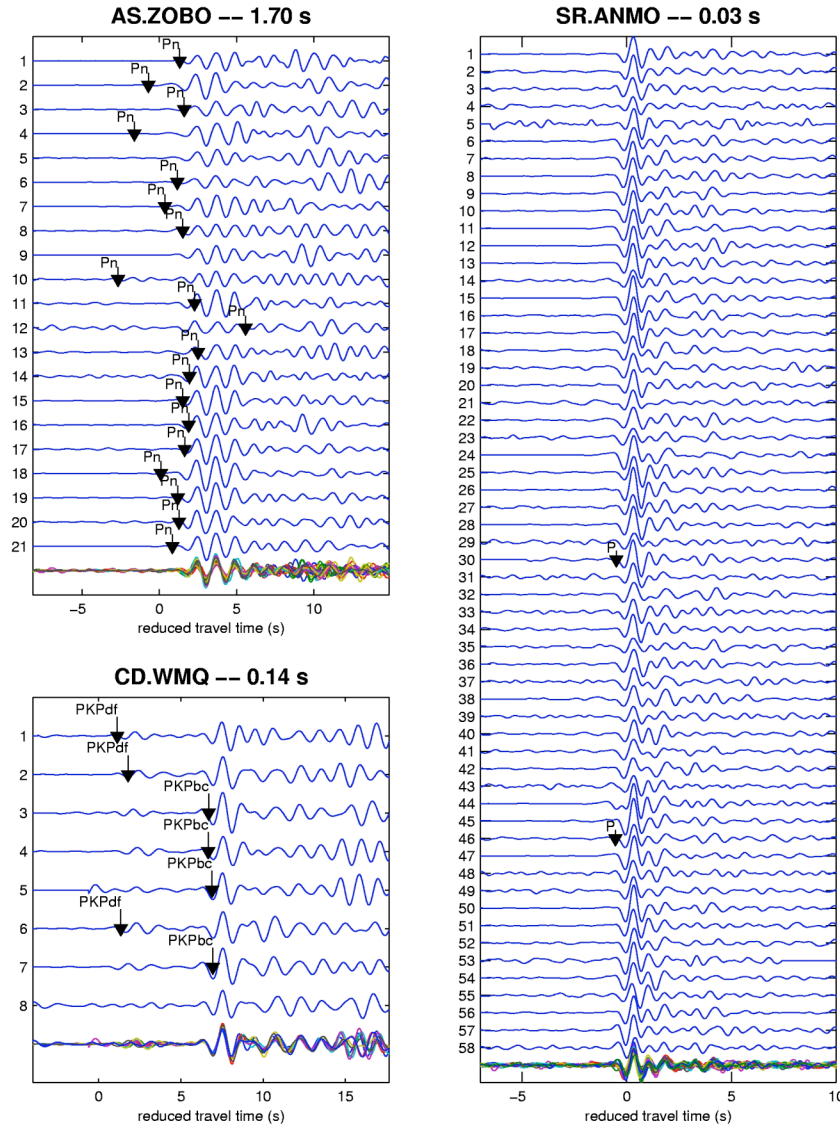
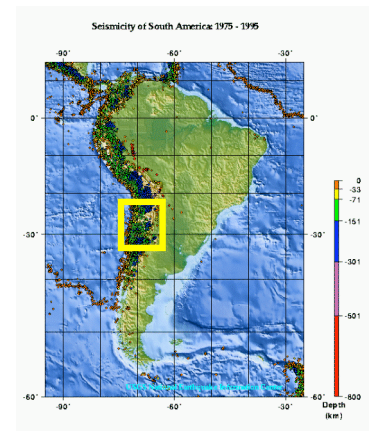


Figure 1 Filtered (0.1-2 Hz) and cross-correlation aligned waveforms of selected events in the Nazca plate beneath Northern Chile (see below) recorded at regional (ZOBO) and teleseismic (ANMO, WMQ) stations. Phases observed at ANMO are bottoming in the lower mantle, those at WMQ in the core. Bottom line in each panel superimposes traces shown above, arrows indicate arrival-time picks available from the EHB bulletin.



We use phase picks and initial locations as listed in the EHB bulletin (Engdahl et al., 1998; Bob Engdahl, pers. comm.). From a total of 11,780 first and later arriving P and S body wave phase picks, 91,783 picks have been pair wise observed at common stations (Figure 2). Ten stations are within local distances (<200 km) from the cluster centroid, most of them locating south of the fault and therefore causing a primary station gap >180° for most of the 75 events. 71 events were recorded at one or more local stations, 37 events at 4 or more local stations. 227 stations are within regional distances (<2000 km), with most stations located in Greece and western Europe. 383 stations recorded the events at teleseismic distances (>2000 km). We have sub-sampled the station distribution for each event pair in order to avoid strong spatial clustering of partial derivatives in areas with dense seismic networks (e.g., arrays or local networks reporting to the ISC). We select only the best station (i.e., the highest quality pick) within bins of 3°x3° beyond a distance of 200 km from the cluster centroid.

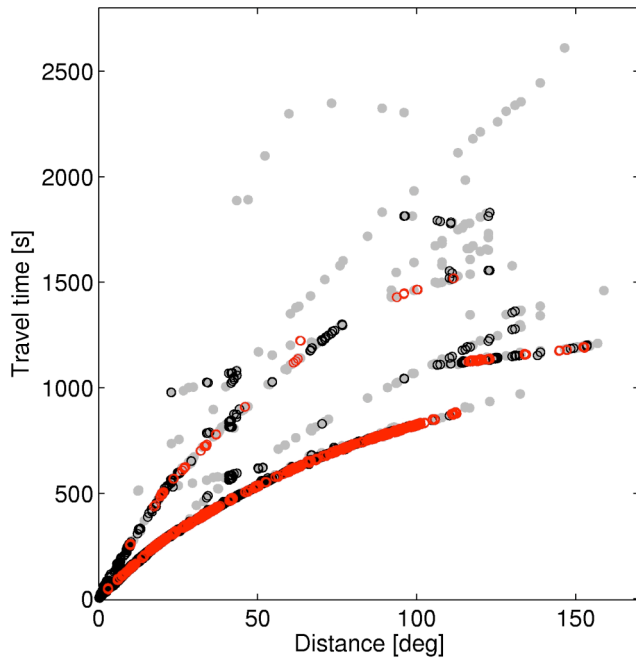


Figure 2 Phase travel times as a function of distance for the 75 earthquakes in the Izmit-Düzce sequence. Gray dots denote original EHB bulletin picks, black circles pairwise observed picks, and red circles phases for which cross correlation measurements were obtained.

In addition to the phase pick data we compute accurate differential times by performing a total of 21,812 cross correlations on 561 filtered (0.1-2 Hz) seismograms obtained from the IRIS DMC, using the time-domain method of Schaff et al. (2004). We choose window lengths of 10 s around the predicted P, PKP, S, and SKS phase arrival time, and searched over lags of 5 s. Similar to the Chile application a STA/LTA filter (1s/5s) is applied to the seismograms before the correlation measurements were carried out. A total of 1,977 P-wave and 49 S-wave correlations had correlation coefficients $CC > 0.7$ (Figure 2). The percentage of similar event pairs is 9% which is less than that for the Chile earthquakes (14%). Most of the events that correlate can be grouped into doublets and triplets. Careful inspection of seismograms for pairs of events that are closely indicate that, even though their hypocenters are close together, the waveforms observed at common stations are dissimilar, suggesting that variation in source mechanisms may be the reason for the low percentage of correlation measurements (see below).

Relocation results

A series of 50 dynamically weighted damped least-square iterations is used to simultaneously relocate the 75 events using the combined pick and correlation data. Interevent distance thresholds are gradually decreased from 180 km during the first to 25 km during the final iterations. We invert for all hypocentral parameters (including depths) except for the depths of the two mainshocks, which we fix at 17 km for the Izmit and 10 km for the Düzce shock. Note that most depths in the EHB catalog are fixed at a default value of 10 km. Before relocation, the number of links established between each event and its neighboring events in the cluster range from 759 to 4046. During relocation the data is reduced by the weighting function to between 73 and 1326 highest quality links per event. The double-difference results are shown in Figure 3 in a map view and three cross sections. Ellipses in Figure 3a and crosses in Figure 3b indicate 90%

confidence levels obtained from a bootstrap analysis of the final double-difference vector. Error ellipses are mostly elongated in north-north-east direction, consistent with a lack of local and regional stations north of the fault. Mean location uncertainties are 3 km laterally and 4 km vertically. Mean horizontal and vertical shifts between the initial (EHB) and relocated locations are 4.5 km and 5.1 km, respectively.

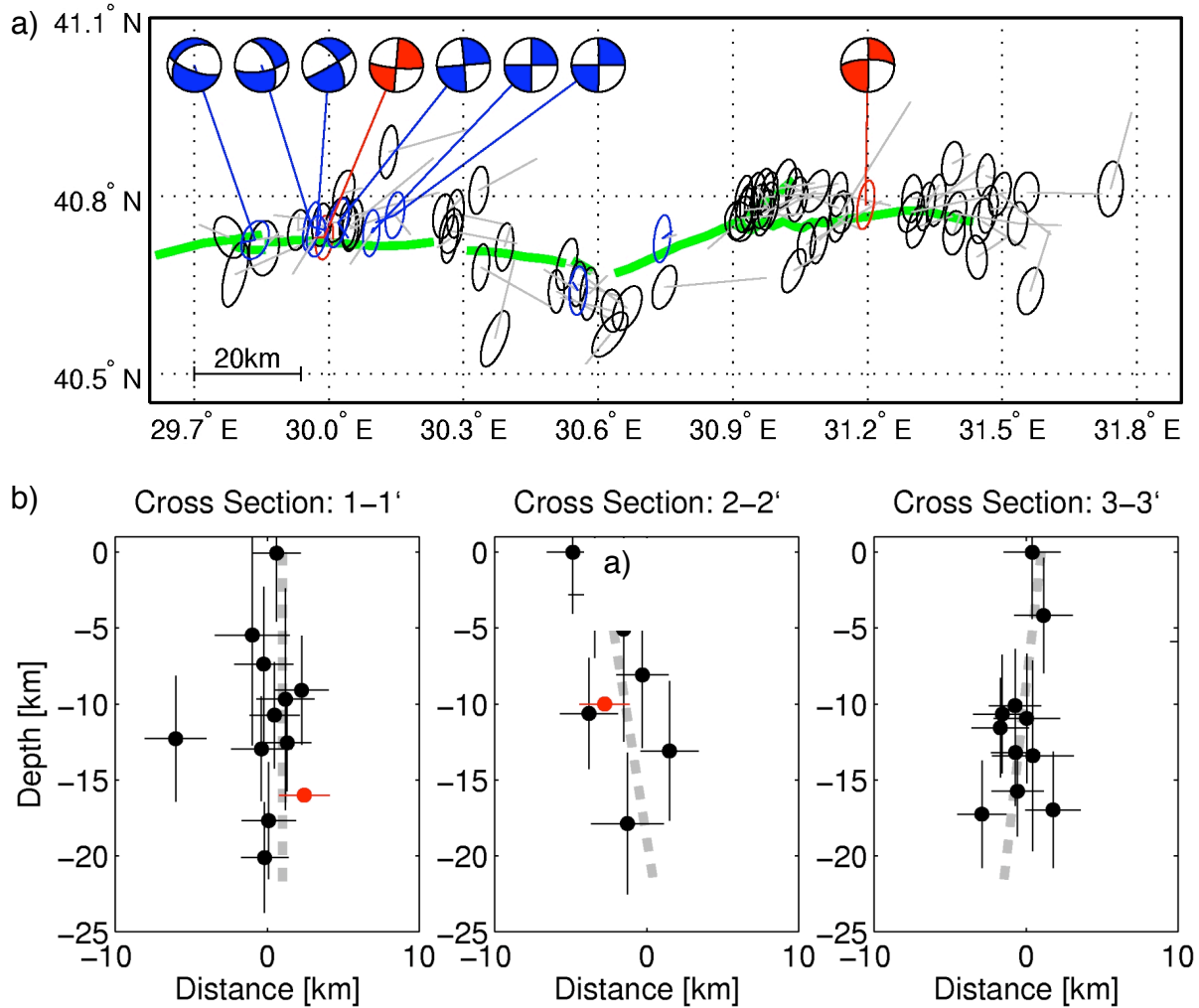


Figure 3 Double-difference locations from pick and cross-correlation data shown in a) map view and b) fault perpendicular cross sections for the 75 events in the Izmit-Düzce sequence. Error estimates at the 90% confidence level are represented by ellipses in (a) and crosses in (b). The Izmit and Düzce mainshocks are shown in red, the GT2 events of Özalaybey et al. (2002) in blue. Gray lines connect DD locations to corresponding initial locations taken from the EHB catalog, red and blue lines to mainshock and GT2 locations, respectively. Focal mechanisms are shown for the two mainshocks (red) (USGS CMT) and for 6 GT2 events (blue) (Özalaybey et al., 2002). Boxes in a) indicate location and orientation of cross sections shown in b). Green line in a) denotes surface trace of the fault rupture (from Pucci et al., 2006). Dashed gray lines in b) represent fault dip inferred from relocated aftershocks.

Evaluation using ground truth data

We evaluate the accuracy of the relocation results with respect to locations of events determined in special studies using dense local networks (Özalaybey et al., 2002) and with respect to near-surface geologic information (Pucci et al., 2006). A detailed study of the Izmit aftershock sequence by Özalaybey et al. (2002) produced an aftershock catalog (RMS = 0.16 s) with average horizontal and vertical errors of 1.7 km and 2.3 km, respectively, rendering them ground truth at the 2 km level (GT2). From a list of 27 well-located larger magnitude aftershocks (Özalaybey et al., 2002, their Table 2), 6 events, located near the mainshock between 29.8 E and 30.2 E., are also among the 75 events studied here. Accurate locations of an additional two events determined from recordings at a local temporary seismic network (N. Seeber and J. Armbruster, pers. communication) are also used for comparison. The first event is an aftershock of the Izmit mainshock and locates at approximately 30.55 E in Figure 3a slightly south of the surface trace. The second is an aftershock of the Düzce mainshock and occurred at 30.75 E close to the fault. Comparing these accurate local network locations with their corresponding double-difference solutions results in mean horizontal and vertical differences of 2.4 km and 1.9 km, respectively. Except for one event, all corresponding 90% coverage ellipses overlap.

A comparison between the double-difference solutions and locations listed in the catalogs of the EDR, ISC, and the EHB are shown in Figure 4a and b. Median (mean) horizontal/vertical differences are 7.2/4.5 (8.6/5.3) km for EDR, 4.8/5.4 (6.4/6.1) km for ISC, and 8.2/4.5 (8.1/5.6) km for EHB locations. Note that most events in the EHB and EDR catalogs have depths fixed at default values. Figure 4c and d show the horizontal and vertical distribution of mislocations for the 9 events relative to the local network solutions of Özalaybey et al. (2002). The median (mean) horizontal mislocation are 3.9 (5.5) km for the EDR, 3.3 (3.3) km for the ISC, and 6.4 (6.8) km for the EHB locations. These values are significantly greater than the median (mean) horizontal mislocation of 2.6 (2.4) km for the double-difference solutions.

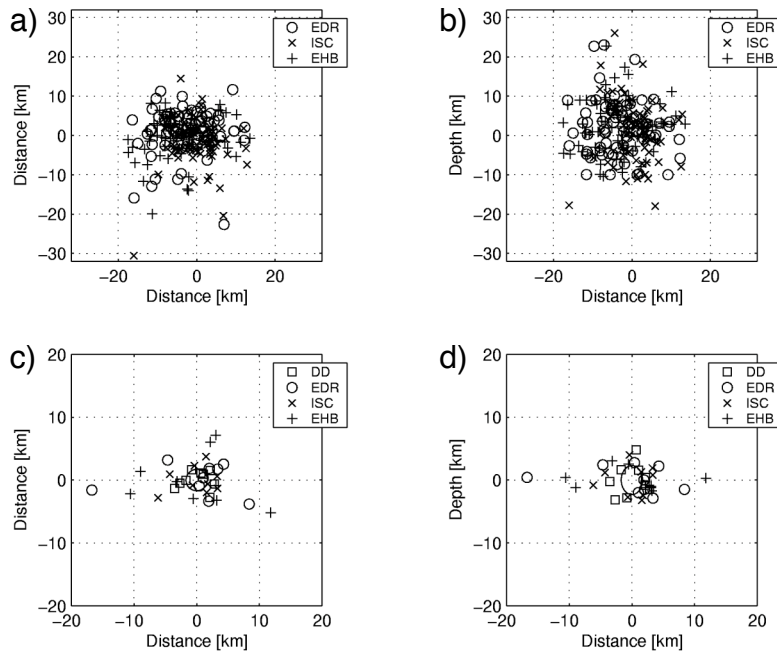


Figure 4 Horizontal (a) and vertical (b) distribution of differences between the 75 DD locations and their corresponding locations listed in the EDR, ISC, and EHB catalogs. Horizontal (c) and vertical (d) differences between the 9 GT2 locations of Özalaybey et al. (2002) and the DD, EDR, EHB, and ISC locations. Ellipses indicate the approximate average error of the GT2 events.

Evaluation using near surface information

The overall pattern of the relocated aftershocks of both the Izmit and Düzce mainshocks correlate with the general trend of the surface trace (Figure 3a). The scatter in the epicenter distribution likely reflects the complex rupture of both events, as evident from surface expressions of the main ruptures (Barka et al., 2002; Akyüz et al., 2002; Pucci et al., 2006) and the variation of focal mechanisms. Relocated aftershocks near the Izmit hypocenter indicate a 20 km deep, near vertical fault (cross section 1-1', Figure 3b) consistent with the focal mechanisms of the mainshock (red, Figure 3a) and those of three aftershocks east of the main shock (blue, Figure 3a; Özalaybey et al., 2002). The width of the seismically imaged fault is not resolvably different from zero. A large variation in focal mechanisms is observed for three aftershocks west of the mainshock.

In a recent study, Pucci et al. (2006), based on detailed geologic mapping, inferred a rather complex structure of the fault associated with the Düzce earthquake sequence. Of particular interest to this study is their finding of a south dipping fault of the Cinarli segment on which the mainshock occurred, and a north dipping fault for the adjacent Yenikoy segment to the west. Their results are consistent with fault perpendicular cross sections of our aftershock locations along these segments. Aftershocks along the Cinarli segment (Figure 3b, cross section 2-2') indicate a 10° south dipping fault, while aftershocks along the Yenikoy segment an approximately 5° north dipping fault (cross section 3-3'). The situation along the Yenikoy segment is complicated as some of the events may have reactivated a strand that ruptured during the Izmit event slightly to the north of the Yenikoy segment.

The general complexity of the fault structure, expressed by the aftershock locations, the variation in focal mechanisms and the complex surface ruptures, appears to be the main reason for the low number of earthquakes with similar waveforms at common stations, and thus the relatively low number of cross-correlation differential time measurements. However, the combination of phase pick and available cross-correlation data is sufficient to resolve relative depths to the extent that we can image strike and dip of active fault planes from aftershock data recorded at global seismic networks.

4. Additional Work Towards Global Near-Real-Time DD Solutions

The work carried out under this grant (07HQGR0044), summarized above and described in detail in Waldhauser and Schaff (2007), was aimed at resolving detailed seismicity structures in global earthquake catalogs such as the one produced by the NEIC. In addition to the work proposed in the original proposal, we used remaining funds to work towards the over-arching goal of using these tools in near-real-time during routine operation at the NEIC to improve the location of new events by relocating them rapidly relative to a high-resolution background catalog. Such a real-time double-difference (DD-RT) procedure has been developed for locally recorded earthquakes under a grant from the Northern CA panel of the NEHRP program, and is currently being tested using earthquakes in Northern California (Waldhauser, 2009, in review with BSSA).

Under the grant that covers this report we have carried out additional work to adapt the local DD-RT procedure for operation on global seismic data as provided by the NEIC. Most importantly, both global cross-correlation and double-difference tools are currently being tested to run in 'black-box' operation on large amount of data. This required the developemnt of efficient outlier detection routines that operate before and during the double-difference inversions. The cross-correlation algorithms are currently being applied to ~20,000 events within

the Sumatra aftershock sequence, building on results from a current NSF funded project to relocate the aftershocks using the NEIC/ISC phase arrival time picks together with a teleseismic DD algorithm.

Support from this grant has also been used to establish new procedure for generating high-resolution catalogs of global background seismicity necessary for real-time DD applications. The procedures currently being developed include double-differencing of the EHB catalog, to which additional events from the ISC catalog are added in a single-event double-difference relocation procedure. Such a catalog can then be used as base catalog for global-scale real-time double-difference relocation. We have been testing such a procedure with aftershocks of the 2008 Wenchuan earthquakes, using a combination of ISC/EHB/NEIC data to build a base catalog. Preliminary results are shown in Figure 5. The general picture of the relocated aftershocks agrees with the background seismicity (blue), locally recorded and DD relocated seismicity for the years 1992-1999 (Yang et al., 2005), and surface expression of active faults in that area. Further work is necessary to estimate location precision and accuracy, and to investigate the ability of these new data to map out the coseismic slip area and image the detailed structure of the fault at seismogenic depths. These parameters are important in the context of immediate evaluation and mitigation of seismic hazards.

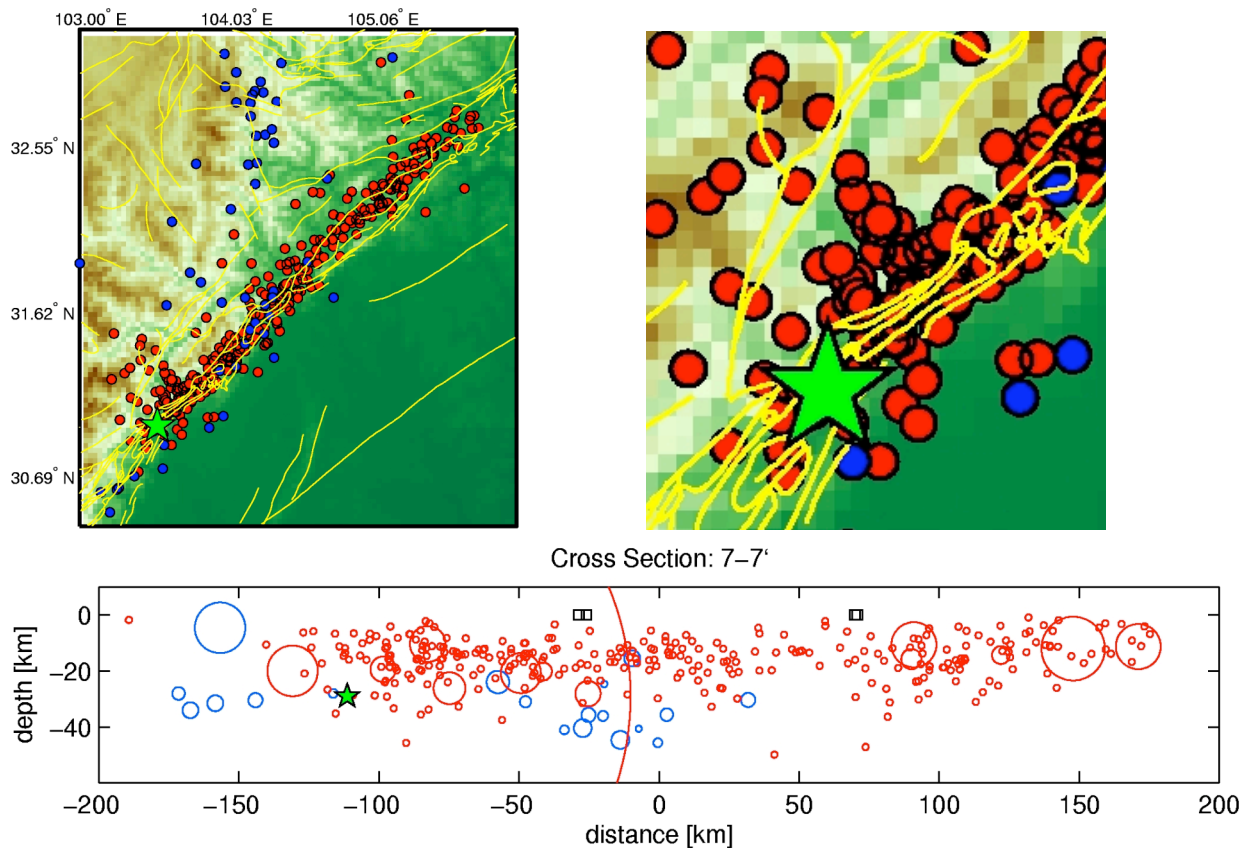


Figure 5 Map view (top panels) and along fault cross section (bottom panel) of preliminary DD relocated aftershocks (red) of the 2008 Wenchuan earthquake (green star). Events 1970-2007 are in blue and are relocated using a combination of EHB and ISC bulletin data. Aftershocks (5/12/2008-6/15/2008) are relocated using NEIC phase picks available on June 16, 2008. Right top panel zooms into the mainshock region.

5. References

- Akyüz, H. S., R. Hartleb, A. Barka, E. Altunel, G. Sunal, B. Meyer, and R. Armijo (2002), Surface Rupture and Slip Distribution of the 12 November 1999 Düzce Earthquake (M 7.1), North Anatolian Fault, Bolu, Turkey, *Bull. Seism. Soc. Am.*, 92, 61-66.
- Barka, A., H. S. Akyüz, E. Altunel, G. Sunal, Z. Çakir, A. Dikbas, B. Yerli, R. Armijo, B. Meyer, J. B. de Chabaliere, T. Rockwell, J. R. Dolan, R. Hartleb, T. Dawson, S. Christofferson, A. Tucker, T. Fumal, R. Langridge, H. Stenner, W. Lettis, J. Bachhuber, and W. Page (2002), The Surface Rupture and Slip Distribution of the 17 August 1999 Izmit Earthquake (M 7.4), North Anatolian Fault, *Bull. Seism. Soc. Am.*, 92, 43-60.
- Engdahl, E.R., R. van der Hilst, & R. Buland, Global teleseismic earthquake relocation with improved travel times and procedures for depth determination, *Bull. Seism. Soc. Am.*, 22, 2317-2320, 1998.
- Özalaybey, S., M. Ergin, M. Aktar, C. Tapirdamaz, F. Biçmen, and A. Yörük (2002), The 1999 Izmit Earthquake Sequence in Turkey: Seismological and Tectonic Aspects, *Bull. Seism. Soc. Am.*, 92, 376-386.
- Poupinet, G., W. L. Ellsworth, and J. Frechet, Monitoring velocity variations in the crust using earthquake doublets: An application to the Calaveras Fault, California, *J. Geophys. Res.*, 89, 5719-5713, 1984.
- Pucci, S., N. Palyvos, C. Zabcı, D. Pantosti, and M. Barchi (2006), Coseismic ruptures and tectonic landforms along the Düzce segment of the North Anatolian Fault Zone (Ms 7.1, November 1999), *J. Geophys. Res.*, 111, B06312, doi:10.1029/2004JB003578.
- Schaff, D. P., G.H.R. Bokelmann, W.L. Ellsworth, E. Zankerka, F. Waldhauser, and G. C. Beroza, Optimizing correlation techniques for improved earthquake location, *Bull. Seism. Soc. Am.*, 94, 705-721, 2004.
- Schaff, D. P., and P. G. Richards, Lg-wave cross correlation and double-difference location: application to the 1999 Xiuyan, China, sequence, *Bull. Seism. Soc. Am.*, 94, 867-879, 2005.
- Schaff, D.P. and F. Waldhauser, Waveform Cross-Correlation-Based Differential Travel-Time Measurements at the Northern California Seismic Network, *Bull. Seism. Soc. Am.*, 95, 2446-2461, 2005.
- Waldhauser, F., and W.L. Ellsworth, A double-difference earthquake location algorithm: method and application to the northern Hayward Fault, California, *Bull. Seism. Soc. Am.*, 90, 1,353-1,368, 2000.
- Waldhauser, F., HypoDD: A computer program to compute double-difference hypocenter locations, *U.S.G.S. open-file report*, 01-113, Menlo Park, California, 2001.
- Waldhauser, F., D. P. Schaff, P.G. Richards, & W.-Y. Kim, Lop Nor revisited: nuclear explosion locations, 1976-1996, from double-difference analysis of regional and teleseismic data, *Bull. Seism. Soc. Am.*, 94, 1879-1889, 2004.
- Waldhauser, F. and D.P. Schaff, Regional and teleseismic double-difference earthquake relocation using waveform cross correlation and global bulletin data, *J. Geophys. Res.*, 112, B12301, doi:10.1029/2007JB004938, 2007.
- Waldhauser, F., Near-real-time double-difference event relocation using long-term seismic archives, with application to Northern California, *Bull. Seism. Soc. Am.*, 2009, in review.
- Yang, Z.X., F. Waldhauser, Y.T. Chen, and P.G. Richards, Double-difference relocation of earthquakes in the central-western China, *J. of Seism.*, 9, 241-264, 2005.

- Zhang, J., X. Song, Y. Li, P.G. Richards, X. Sun, & F. Waldhauser, Inner core differential motion confirmed by earthquake waveform doublets, *Science*, 309, 1357-1360, 2005.
- Zhang, J., F. Waldhauser, P.G. Richards, and D.P. Schaff, Double-difference relocation of an earthquake nest at Bucaramanga, Colombia: Revelation of a vertical fault at intermediate depth, SSA Annual Meeting, Hawaii, *Seism. Res. Lett.*, 78(2), 2007.

6. Papers/abstracts published related to this project

- Waldhauser, F. and D.P. Schaff, Regional and teleseismic double-difference earthquake relocation using waveform cross correlation and global bulletin data, *J. Geophys. Res.*, 112, B12301, doi:10.1029/2007JB004938, 2007.
- Waldhauser, F. and D. Schaff, Seismic monitoring using long-term archives: New directions and opportunities, Bi-Lateral Workshop Under the Sino-US Earthquake Studies Protocol, Boulder, CO, Nov. 11-14, 2008.
- Waldhauser, F. and D. Schaff, Back to the future: Long-term seismic archives re-visited, *Eos. Trans. AGU*, 88(52), Fall Meet. Suppl., Abstract U23C-1447, 2007.
- Zhang, J., F. Waldhauser, P.G. Richards, and D.P. Schaff, Double-difference relocation of an earthquake nest at Bucaramanga, Colombia: Revelation of a vertical fault at intermediate depth, SSA Annual Meeting, Hawaii, *Seism. Res. Lett.*, 78(2), 2007.